Direct observation of DNA overwinding by reverse gyrase

Taisaku Ogawa[a], Katsunori Yogo[a,1], Shou Furuike[a,2], Kazuo Sutoh[a], Akihiko Kikuchi[b], and Kazuhiko Kinosita Jr.[a,3]

[a]Department of Physics, Faculty of Science and Engineering, Waseda University, Shinjuku-ku, Tokyo 169-8555, Japan; and [b]Division of Molecular Mycology and Medicine, Nagoya University Graduate School of Medicine, Nagoya 466-8550, Japan

Edited by James M. Berger, Johns Hopkins University School of Medicine, Baltimore, MD, and approved April 27, 2015 (received for review November 20, 2014)

Reverse gyrase, found in hyperthermophiles, is the only enzyme known to overwind (introduce positive supercoils into) DNA. The ATP-dependent activity, detected at >70 °C, has so far been studied solely by gel electrophoresis; thus, the reaction dynamics remain obscure. Here, we image the overwinding reaction at 71 °C under a microscope, using DNA containing consecutive 30 mismatched base pairs that serve as a well-defined substrate site. A single reverse gyrase molecule processively winds the DNA for >100 turns. Bound enzyme shows moderate temperature dependence, retaining significant activity down to 50 °C. The unloaded reaction rate at 71 °C exceeds five turns per second, which is $>10^2$-fold higher than hitherto indicated but lower than the measured ATPase rate of 20 s^{-1}, indicating loose coupling. The overwinding reaction sharply slows down as the torsional stress accumulates in DNA and ceases at stress of mere ∼5 pN·nm, where one more turn would cost only sixfold the thermal energy. The enzyme would thus keep DNA in a slightly overwound state to protect, but not overprotect, the genome of hyperthermophiles against thermal melting. Overwinding activity is also highly sensitive to DNA tension, with an effective interaction length exceeding the size of reverse gyrase, implying requirement for slack DNA. All results point to the mechanism where strand passage relying on thermal motions, as in topoisomerase IA, is actively but loosely biased toward overwinding.

reverse gyrase | topoisomerase | magnetic tweezers | DNA overwinding | torsion

Reverse gyrase, discovered in 1984 in a hyperthermophilic archaeon *Sulfolobus* (1) which was later classified as *Sulfolobus tokodaii* (2), is a unique DNA topoisomerase that can introduce positive supercoils into DNA (3–7). The only other enzyme that has the gyration activity is DNA gyrase, which introduces negative supercoils. Although DNA gyrase belongs to type II topoisomerase, which changes the linking number (Lk) of dsDNA by two by cutting and religating both strands simultaneously, reverse gyrase is of type IA topoisomerase (topo IA), where one strand is cut to allow the passage of the other, resulting in the Lk changes in steps of one (3–7). Reverse gyrase is found in hyperthermophilic archaea and eubacteria, and the positive supercoiling activity requires a temperature above 70 °C (8, 9). The enzyme is a 130-kDa single polypeptide, a fusion complex of two domains (10): The carboxyl terminal half is related to topo IA, whereas the amino terminal half has an ATP-binding site and is akin to helicase, although neither the whole enzyme nor the isolated helicase-like domain shows genuine helicase activity (11). A crystal structure of the full-length reverse gyrase (12) and more recent structures with additional features (13) all support the basic two-domain construct. The physiological roles of reverse gyrase are not yet fully clear, although positive supercoiling is expected to protect DNA from denaturation at the growth temperatures of hyperthermophiles.

Reactions of reverse gyrase have so far been analyzed in bulk assays on circular (plasmid) DNA. Basically, the enzyme only increases the Lk of DNA: relaxation of negatively supercoiled DNA, which does not require ATP and is rapid, and an ATP-dependent slower introduction of positive supercoils (14, 15). Single-stranded (ss) regions in DNA are required for binding and positive supercoiling (16, 17). The supercoiling activity depends on the enzyme-to-DNA ratio, requiring a molar ratio of more than 10 for effective activity (15). However, when an ss bubble (continuous base pair mismatches) or an AT-rich sequence more than 20 bp long was inserted in a DNA substrate, the positive supercoiling activity became detectable at substoichiometric ratios (17). Positive supercoiling requires ATP, but the coupling appears loose in that many ATP molecules are hydrolyzed per introduced turn (18).

The mechanism of positive supercoiling has been discussed on the basis of the two distinct topo IA and helicase-like domains and a "latch" in between that appears to lock the topo IA domain in a closed conformation (12). Strand passage likely takes place in the topo IA domain, and the passage must somehow be biased toward overwinding with the energy supplied by ATP hydrolysis. The helicase-like domain alters its affinity for dsDNA and ssDNA depending on the bound nucleotide (7), hinting at how ATP hydrolysis is coupled. However, crucial information, such as the processivity, individual kinetics, and overwinding torque, is still scarce. The activity inferred from bulk studies is quite low (17, 18), at most on the order of one superhelical turn per minute, which might be limited by the assay methods.

Motivated by recent single-molecule studies that have revealed the operation of various topoisomerases in real time (19–23), we have observed the activity of purified reverse gyrase from *S. tokodaii* (4) under an optical microscope at 71 °C (Fig. 1). A magnetic bead was tethered to a glass surface with linear dsDNA. When reverse gyrase overwound the DNA, the bead rotated, or sank when rotation was constrained. Inclusion of an ss bubble in

Significance

Reverse gyrase resides in bacteria that live in hot conditions. The enzyme further intertwines the double helix of DNA to make it tighter. In biochemical assays, reverse gyrase appears quite inefficient, requiring many enzyme molecules per DNA and yet taking many minutes to wind it up. Here, we show that one reverse gyrase molecule rapidly overwinds relaxed DNA but begins to idle as torsion accumulates. Excess torsion would hamper replication/transcription activities, whereas quick restoration of modest torsion prevents thermal denaturation of DNA. We discuss how reverse gyrase lets one strand of DNA pass the other in a preferred direction to achieve overwinding.

Author contributions: T.O. and K.K. designed research; T.O. performed research; K.Y., S.F., and K.S. contributed new reagents/analytic tools; A.K. prepared reverse gyrase; T.O. analyzed data; and T.O., A.K., and K.K. wrote the paper.

The authors declare no conflict of interest.

This article is a PNAS Direct Submission.

Freely available online through the PNAS open access option.

[1]Present address: Graduate School of Medical Sciences, Kitasato University, Sagamihara, Kanagawa 252-0373, Japan.

[2]Present address: Department of Physics, Osaka Medical College, Takatsuki 569-8686, Japan.

[3]To whom correspondence should be addressed. Email: kazuhiko@waseda.jp.

This article contains supporting information online at www.pnas.org/lookup/suppl/doi:10.1073/pnas.1422203112/-/DCSupplemental.

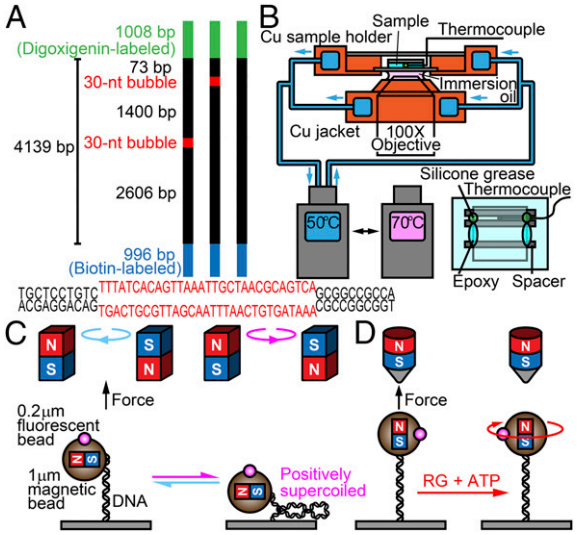

Fig. 1. Experimental design. (*A*) DNA constructs. (*Bottom*) Bubble sequence is shown. (*B*) Temperature control. (*Bottom Right*) Top view of a sample chamber. (*C*) Selection of DNA under a magnet pair. The bead, with a preferred axis for magnetization, must be on the side of the DNA, and the bead must sink when it is rotated in the overwinding direction. N, North; S, South. (*D*) Observation of DNA overwinding reaction by reverse gyrase under a single magnet, which allows free rotation of the bead. The bead rotates to relax the torsional stress in DNA introduced by reverse gyrase (RG).

the DNA greatly enhanced the activity, which we analyze to infer the underlying mechanism.

Results

Real-Time Observation of DNA Overwinding Activity. We prepared three kinds of linear DNA substrates, two with a bubble 30 nt long at different (middle and end) positions and one without a bubble (Fig. 1*A*; details in Fig. S1). One end of the DNA was attached to the coverslip surface through biotin-streptavidin linkages, and the other end was attached to a 1-μm magnetic bead through digoxigenin/antidigoxigenin antibody linkages. Small fluorescent beads were attached to the magnetic bead to facilitate observation of rotation. After infusing reverse gyrase in a medium containing 5 mM ATP and 10 mM $MgCl_2$, the sample was set on an inverted microscope and the temperature was controlled to within ±1 °C as monitored with a thermocouple placed next to the sample (Fig. 1*B*).

We started an assay by searching at 50 °C for a bead to be analyzed that satisfied the following conditions:

i) The number of fluorescent daughter beads had to be one or two for unambiguous tracing of rotation.

ii) The magnetic bead had to be tethered by one unnicked DNA molecule. For this selection, we used a horizontal pair of magnets to pull the bead upward at 0.5–0.9 pN and rotated the bead for 30 turns in the overwinding (counterclockwise as viewed from above) direction. This operation should lower the bead (Fig. 1*C*); otherwise, the DNA is nicked. Rotation in the opposite (unwinding) direction, in contrast, should not lower the bead appreciably at this relatively high tension (24), unless the bead is tethered by two or more DNA molecules. The latter unwinding test, however, was postponed until all measurements in an observation chamber were finished, because unwinding might lead to excess binding of reverse gyrase. In fact, we never encountered the case of multiple tethering because the surface density of DNA was low, such that only several beads were observed in the field of view measuring 49 × 65 μm^2.

iii) The magnetic bead must be on a side of DNA in the horizontal field in test *ii* (Fig. 1*C*), because we were to apply a vertical magnetic field for the reverse gyrase assay (Fig. 1*D*). Thus, we selected a bead of which the center itself rotated along a large circular orbit, deselecting those beads that rotated only on their own axis. After the rotation test, we wound back the bead for 30 turns to relax the DNA. On average, one bead in ~10 fields of view passed the three tests.

Once a candidate bead was found, we replaced the horizontal magnets with a vertical magnet (Fig. 1*D*) to pull the bead upward at 0.5 pN while allowing free rotation. After confirming the bead to rotate (or to undergo rotational diffusion) nearly on its own axis, we turned on fluorescence excitation and started the observation for analysis for 5 min at 50(±1) °C, followed by another 5 min at a higher temperature and 5 min at 50 °C again. At the end, we repeated test *ii* above. About 10% was found to be nicked by this time, and we discarded such data. We then searched for another bead in the same chamber, starting with test *i* above. Typically, one chamber was on the heating stage for 2–3 h, and not for more than 3 h, during which time three to 10 beads were recorded for detailed analysis.

Overwinding Activity Leads to Indefinite Rotations. At 71 °C and with 10 nM reverse gyrase, beads tethered by the three different DNA substrates all rotated clockwise when viewed from above (Fig. 2). This direction is as expected for overwinding of the right-handed DNA double helix by reverse gyrase, because the bead at the free end should rotate to relax the overwound state. At 10 nM enzyme, the rotation continued indefinitely: We never observed a conspicuous long (>100 s) pause except for complete cessation of rotation due to DNA nicking. Such an unlimited rotation is not possible with circular DNA (unless nicked).

The significant overwinding of the nonbubble DNA is accounted for by the presence of AT-rich sequences in the substrate (AT content per 20 bp reaches 80% or 85% in eight stretches each sized 20–35 bp). With the bubble, the rotation was much faster at 71 °C: 0.23 ± 0.03 revolutions per second (rps) (mean ± SD for n = 8 beads; all errors in this paper are SDs) for mid-bubble and 0.27 ± 0.07 rps for end bubble (n = 11), compared with 0.079 ± 0.028 rps for nonbubble DNA (n = 9). Bulk observation (17) has also shown that a bubble greatly promotes the reverse

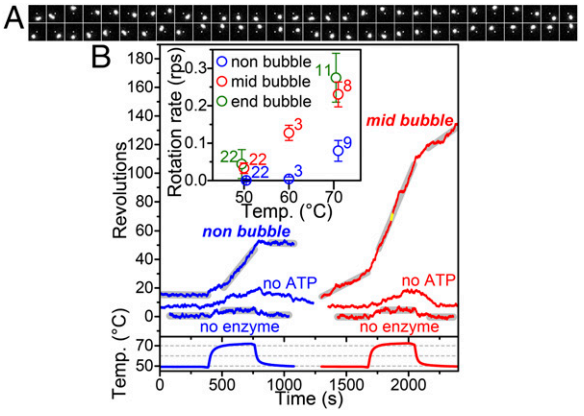

Fig. 2. Overwinding of DNA by reverse gyrase leads to indefinite rotations. (*A*) Sequential images at 132-ms intervals of a fluorescent daughter bead attached to a tethered magnetic bead. White dots show the center of rotation. View from above in Fig. 1*D*. The image size is 2.8 × 2.8 μm^2. The images are from the yellow portion of the red curve in *B*. Also see Movie S1. (*B*) Time courses of bead rotation at 10 nM reverse gyrase and monitored sample temperature. Thick straight lines show the linear fit to the portion within ±1 °C of 50 °C or 71 °C, from which the average rotary speed is calculated. (*Inset*) Temperature dependence of the average rotary speeds at 10 nM reverse gyrase under DNA tension of 0.5 pN. Numbers are n (beads examined; approximately twice the number of beads for 50 °C, where the second measurement occasionally failed), and error bars show SD.

gyrase activity. Our results, in addition, demonstrate that reverse gyrase can overwind DNA even at 50 °C, albeit slowly, where bulk activity has not been reported. The temperature dependence for bubbled substrates (Fig. 2*B*, *Inset*) is moderate and gradual, and it is independent of the position of the bubble. In contrast, we did not observe unidirectional rotation with the nonbubble DNA at 60 °C or below. Thermal melting is negligible at 60 °C, and an ss region needed for reverse gyrase binding is virtually absent. Even at 71 °C, ss regions created by thermal melting should be transient and unstable, and the separated strands may not be long enough for efficient strand passage. A stable bubble would thus warrant a faster reaction.

We show below that the activity of reverse gyrase is highly sensitive to the tension and torsional stress in DNA. The results shown in Figs. 2 and 3 were all under 0.5 pN of tension. Torsional stress is determined by the viscous friction against the rotating bead and is given by $\pi D^3 \eta \omega$, where D is the bead diameter, η is the viscosity of water, and ω is the bead rotation speed in radians per second. For the mid-bubble DNA, the stress was 1.8 pN·nm at 71 °C (0.36 pN·nm at 50 °C), and for the nonbubble DNA, it was 0.62 pN·nm at 71 °C. Reverse gyrase worked against this much counteracting torque.

In the absence of the enzyme, we observed only Brownian rotations of the bead, with rms excursions of 290 ± 50° (5 min each for six beads) at 71 °C and 290 ± 40° at 50 °C (n = 10) for the nonbubble DNA. These values for the DNA contour length of ∼1.4 μm imply a torsional persistence length of 55 nm and are commensurate with the torsional elasticity of B-form DNA (25). We also note that heating from 50 to 71 °C in the absence of reverse gyrase resulted in a clockwise rotation of 3.5 ± 0.7 revolutions (n = 6) as seen at the bottom of Fig. 2*B*. This finding is consistent with the reported unwinding rate of $-0.0105°\cdot°C^{-1}\cdot bp^{-1}$ covering this temperature range (26). The presence of a bubble changed these values only slightly (analyzed for the mid-bubble): Fluctuations were 410 ± 40° (n = 4) at 71 °C and 290 ± 50° (n = 7) at 50 °C, and the thermal unwinding from 50 to 71 °C was 4.5 ± 1.2 revolutions (n = 4). The effects of the bubble on the physical properties of DNA appear localized.

Without ATP, reverse gyrase gradually unwound DNA at 71 °C, and the unwinding was slowly reversed upon cooling (Fig. 2*B*, *Middle*; longer records are shown in Fig. S2). Presumably, reverse gyrase binds to where DNA happens to melt, with such occurring in succession because bead rotation keeps the DNA relaxed. In the presence of ATP, in contrast, reverse gyrase continually overwinds DNA, hindering melting and preventing excess binding of reverse gyrase. Indeed, we observed little reverse rotation upon cooling to 50 °C (Fig. 2*B*, *Top* and Fig. S2). As expected, unwinding of circular plasmids in the absence of ATP requires nicking (27).

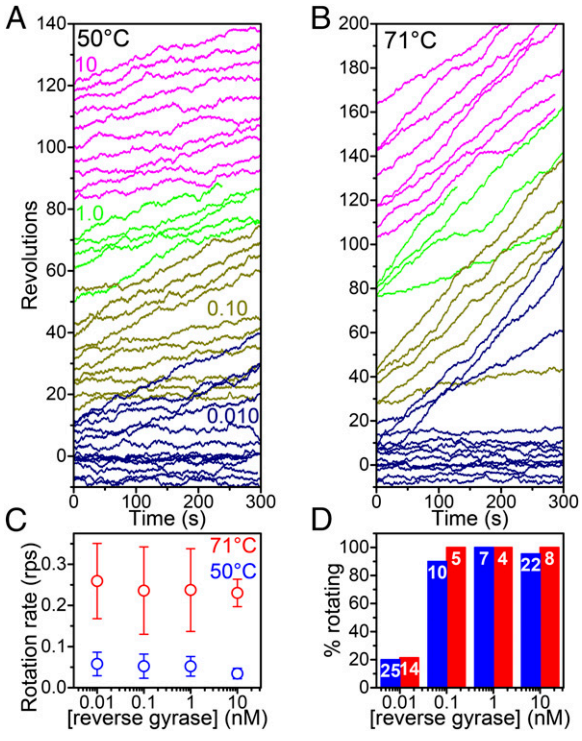

Fig. 3. Concentration dependence of overwinding activity at 0.5 pN of tension. (*A* and *B*) Rotation time courses at two temperatures. Colored numbers show [reverse gyrase] in nM. (*C* and *D*) [Reverse gyrase] dependence of the rotary speed (*C*) and the probability of rotation (*D*). Curves in *A* and *B*, with additional data to include all beads that satisfied conditions *i–iii* in the main text, are each fitted with a straight line to give individual rotary speeds, which are classified as rotating (>0.01 rps) or nonrotating (<0.01 rps). The average speed of rotating beads is shown in *C*, with error bars showing SD. Numbers in *D* show the total beads analyzed (71 °C) or approximately twice the number of beads (50 °C; data from 50-60-50 °C measurements are included).

Reverse Gyrase Works Processively. To gain insight into the mechanism of strand passage, we focus below on the mid-bubble substrate. The ss region needed for binding and strand passage is well defined and preserved in the bubble, compared with thermally induced binding sites where base pairs are broken and reformed dynamically. The end bubble gave indistinguishable behaviors, but we avoid possible complication due to the nearby bead.

To see whether the observed continuous rotation was effected by successive operations of many reverse gyrase molecules, we decreased the enzyme concentration into the picomolar range (Fig. 3). Both at 50 °C and 71 °C, we did not notice an appreciable difference in rotation behaviors until we went down to 0.1 nM, below which finding a rotating bead became difficult. Those beads that did rotate, however, rotated at speeds indistinguishable from the speed at 10 nM. The implication is that one reverse gyrase stays on the bubble for hundreds of seconds [dissociation rate (k_{off}) < 10^{-2} s^{-1}], introducing many positive turns (>100 on average at least at 71 °C) processively. The average speed was 0.24 ± 0.07 rps (n = 20 for all reverse gyrase concentrations) at 71 °C and 0.046 ± 0.022 rps (n = 39) at 50 °C, which we interpret as the catalytic rate of the bound enzyme under DNA tension of 0.5 pN and counteracting torque of 1.9 pN·nm (71 °C) or 0.50 pN·nm (50 °C). The rate increases 5.2-fold per 21 °C, corresponding to the temperature coefficient Q_{10} of 2.2, which is within the range for usual enzymes. To some extent, the rotary rate varied from bead to bead (Fig. 3 *A* and *B*) for an unknown reason; however, the concentration dependence argues against the possibility that faster rotations were driven by two or more enzyme molecules.

From Fig. 3*D*, we estimate the dissociation constant, K_d, of reverse gyrase for the bubble to be roughly 30 pM (between 10 and 100 pM) both at 50 °C and 71 °C. The high affinity is commensurate with the low k_{off} above. At 50 °C, some of the rotation time courses appear to be punctuated with pauses on the order of ∼100 s (shorter pauses may also exist at 71 °C), although Brownian fluctuations hamper clear distinction. If the pauses are real, reverse gyrase tends to work in a stop-and-go fashion at low temperatures while clinging to the bubble; the pauses are unlikely to represent dissociation and rebinding of the enzyme, because pausing patterns are similar at high- and low-enzyme concentrations and, at 10 pM in particular, rebinding within 100 s would imply too high a binding rate (k_{on}) exceeding 10^9 $M^{-1}\cdot s^{-1}$.

Plectoneme Formation by Reverse Gyrase. In the experiments above, torsional stress remained low thanks to bead rotation. To see the effect of torsion, we used horizontal magnets to prevent bead rotation (Fig. 4*A*). Overwinding by reverse gyrase would then introduce plectonemes in the DNA, and the bead would sink toward the bottom, as was indeed observed. Formation of plectonemes

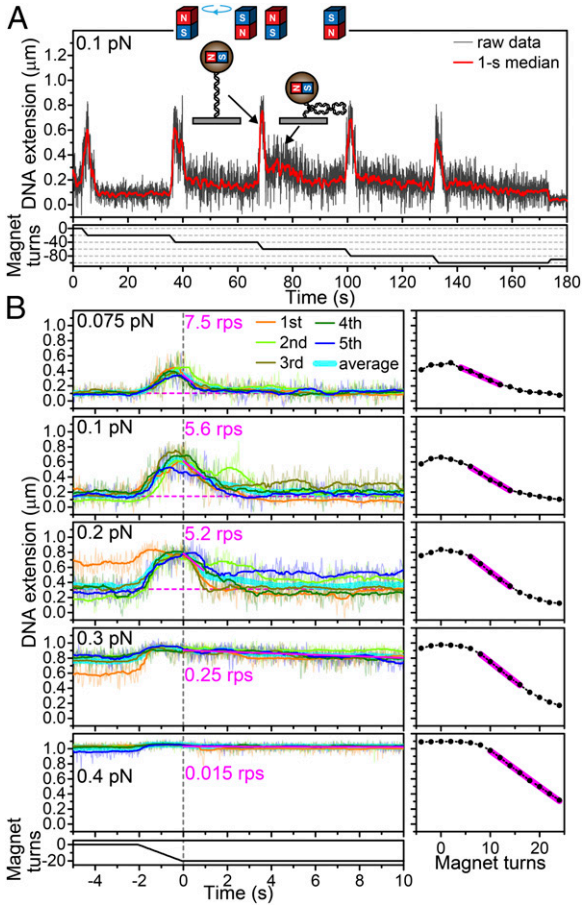

Fig. 4. Plectoneme formation by reverse gyrase. (*A*) Repetitive bead sinking in response to unwinding magnet rotation at 0.1 nM reverse gyrase. Unwinding magnet turns are taken as negative. After several trials under the same tension, we rotated the magnets in the overwinding direction to let the bead sink close to the surface (end of the curve). We then changed the tension and repeated the same procedure. (*B*, *Left*) Sinking time courses at various tensions for the bead in *A*. Individual time courses distinguished by colors are first 1-s median-filtered (smoother curves), aligned at the end of unwinding rotation (time 0), and averaged (thick cyan curve). At ≤0.2 pN, where sinking is significant, we fit the average with the magenta line between 0 s and the midpoint of sinking, with the final level (magenta dashed line) being estimated at 24–29 s; at ≥0.3 pN, the fit is between 0 and 10 s. Magenta numbers show estimated overwinding rates. (*B*, *Right*) Bead sinking by magnet rotation in the absence of reverse gyrase. Magenta lines show linear fit (also see Fig. S3).

requires a certain torque that depends on the tension on DNA; thus, we learn how much torque reverse gyrase can generate.

This supercoiling experiment was done at 71 °C, without the fluorescent daughter beads. We set the sample on the hot stage and waited for temperature equilibration, during which time the beads that would sink (tethered by unnicked DNA) already sank. We first rotated the magnets in the unwinding direction to raise the beads. We selected those beads that rotated around their own axis (i.e., those beads that were above the DNA) (Fig. 4*A*). We estimated the bead height (DNA extension) by deliberately defocusing the bead image and measuring the size of the diffraction ring (Fig. S3*A*). Because we observed the height rather than the orientation of the bead, fluctuations of the bead did not seriously hamper the analysis; thus, we were able to reduce DNA tension. In fact, we observed bead sinking only at tensions below ~0.3 pN and none at 0.4 pN. After 30–60 s, we rotated the bead 20 turns at 10 rps in the unwinding direction, which brought the bead back to the original height. Unwinding by 30 turns did not change results. Excess underwinding would be rapidly relaxed by reverse gyrase. In this way, we could repeatedly observe bead sinking for the same bead/DNA pair (Fig. 4*A*). Because individual sinking records varied considerably among successive trials, we averaged five to 10 successive runs under the same tension, taking the end of the unwinding maneuver as time 0 (thick cyan lines in Fig. 4*B*).

To convert the observed change in DNA extension into the number of overwinding turns introduced by reverse gyrase, we rotated the bead by magnets in small steps in the absence of reverse gyrase (Fig. 4*B*, *Right* and Fig. S3). The results at 71 °C are qualitatively similar to the results at room temperature (28). Starting from a relaxed DNA with m, the imposed number of turns, of zero, the extension z decreases with m initially slowly until a first plectoneme loop is formed. Thereafter, z decreases linearly as additional loops are introduced to keep the torsional stress in DNA constant. The decrease slows down again as z approaches zero, presumably because the DNA beneath serves as a cushion. We use the slope dz/dm in the linear portion (magenta lines in Fig. 4*B*, *Right*) to estimate the activity of reverse gyrase. In the sinking curves observed in the presence of reverse gyrase (Fig. 4*B*, *Left*), we would expect, after a small lag for the first several turns, a decrease of z at a constant rate. The initial lag, however, was not discerned because reverse gyrase works fast while the torsional stress is low (see below). We therefore took the initial slope, dz/dt, where t is time, of the average sinking curve (cyan lines in Fig. 4*B*, *Left*) as the sinking rate. Division by dz/dm gives dm/dt, the activity in revolutions per second during the plectoneme growth phase. The results at 0.1 nM and 1 nM reverse gyrase are summarized in Fig. 5*A*. The trend suggests that single reverse gyrase works at >5 rps in the absence of tension and torsional stress. Comparison of Fig. 4*B* (*Left* vs. *Right*) indicates that reverse gyrase can introduce up to 10—20 positive supercoils in this DNA with Lk_0, Lk at relaxed state, of ~400. The Lk density $\sigma = \Delta Lk/Lk_0$ reaches +0.025 ~ +0.05, consistent with biochemical assays (see below).

Dependence on Tension and Torsional Stress in DNA. We varied tension to obtain Fig. 5*A*, but torque also varied simultaneously. The torque needed for plectoneme growth can be estimated from the DNA extension vs. rotation curves in Fig. 4*B* (*Right*). Mosconi et al. (28) have shown that their extension-rotation curves under various tension and salt conditions can all be approximated by one simple equation developed by Clauvelin et al. (29), which reads $\Gamma = 2F(dz/dm)L_0/3\pi z_0$, where Γ is the torque for plectoneme growth, F is the tension, dz/dm is the slope in the linear part, L_0 is the contour length of DNA, and z_0 is the extension at $m = 0$. We take L_0 as 1,400 nm and estimate dz/dm and z_0 from Fig. 4*B* (*Right*) and Fig. S3*C* to obtain Γ. In Fig. 5*B*, we replot Fig. 5*A* against Γ. We also include the free rotation result at F = 0.5 pN and Γ = 1.9 pN·nm (orange square in Fig. 5 *A* and *B*). The two panels in Fig. 5 *A* and *B* show the same data, where the effects of tension and torque are convolved. Below, we try to differentiate between the two effects.

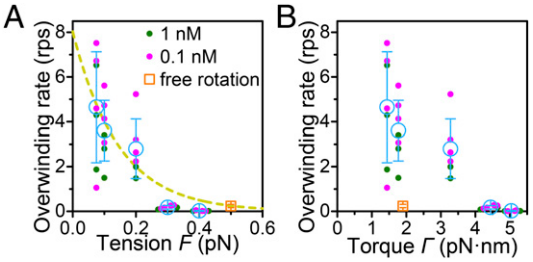

Fig. 5. Overwinding activity plotted against DNA tension F (*A*) and torque Γ required for plectoneme growth (*B*). Dots represent individual beads; circles represent their average, with error bars showing SD; and squares represent free rotation results from Fig. 3*C*. The dashed line in *A* shows the fit with $\exp(-F\delta/k_BT)$.

In Fig. 5*A*, the overwinding rate is zero at 0.4 pN, but tension cannot be the reason why because finite activity is observed at 0.5 pN (orange square in Fig. 5*A*). The decisive factor is torque (Fig. 5*B*): Reverse gyrase ceases to overwind DNA when opposed by a critical torque Γ_c of ~5 pN·nm. Twisting DNA by one revolution against Γ_c would cost $2\pi\Gamma_c \sim 30$ pN·nm of work, which is only sixfold the thermal energy and one-third to one-fourth of the free energy obtained by hydrolyzing one ATP molecule. This is the maximal work reverse gyrase can do in a productive catalytic cycle.

The activity sharply depends on torque only near Γ_c. In Fig. 5*B*, the activity drops more than an order of magnitude between 3.3 and 4.4 pN·nm, but the torque dependence is quite moderate below 3.3 pN·nm; note that tension must also contribute to the decrease in activity. Then, if we neglect in Fig. 5*A* the two points at 0.3 and 0.4 pN (4.4 and 5.0 pN·nm of torque), the other four points, including the orange one, would represent, roughly, the tension dependence alone. The four points can be fitted (dashed line in Fig. 5*A*) with an Arrhenius dependence, $\exp(-F\delta/k_BT)$, giving an interaction length δ of ~32 nm ($k_BT = 4.7$ pN·nm for $T = 344$ K). The two points at 0.1 and 0.5 pN, in particular, are nearly at the same torque of ~1.9 pN·nm (Fig. 5*B*), suggesting that the fit indeed approximates tension dependence. Tension dependence is continuous, although strong with the large δ, whereas torque impedes only near Γ_c and completely blocks net overwinding at Γ_c.

Hydrolysis of ATP. To see if overwinding activity is tightly coupled with ATP hydrolysis, we measured the rate of ATP hydrolysis in bulk solution (Fig. 6 and Fig. S4). At 71 °C, significant hydrolysis occurred without reverse gyrase. Reverse gyrase alone showed little hydrolysis activity, but DNA promoted hydrolysis. The hydrolysis activity with bubbled DNA was 20 s^{-1}, more than twice the estimated overwinding activity at no load (Fig. 5*A*), indicating loose coupling as previously reported (18).

Discussion

Microscopic imaging and manipulation at the high temperatures are far more difficult than at room temperature. Severe drifts limit precision. The sample must not contain heat-labile components, and, even then, the measurement is a race against thermal deterioration. We have partially solved these problems and shown that reverse gyrase works $>10^2$ faster than hitherto indicated in bulk assays. In a bulk assay (17) with a 3.1-kbp bubbled plasmid (Lk_0 of ~300), the product with the highest ΔLk of ~+10 began to appear by 15 min but not at 7 min, when 4 nM reverse gyrase was mixed with 8 nM DNA at 80 °C, indicating an activity of ~10 turns per 10 min per 0.5 enzyme/DNA, or ~0.03 rps at 80 °C. Our direct observation at 71 °C, in contrast, shows that the activity is at least ~5 rps (Fig. 5*A*).

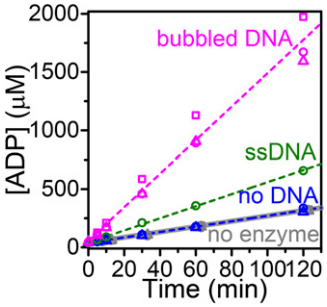

Fig. 6. DNA-dependent ATPase activity of reverse gyrase at 71 °C. Reverse gyrase (10 nM) was incubated with 5 mM ATP and 100 nM DNA (147-nt ssDNA or dsDNA containing a bubble). Each time course with a different symbol was fitted with a line to obtain an individual rate, although averaged lines are shown here. The hydrolysis rate without enzyme was 2.3 ± 0.1 μM·min^{-1} ($n = 3$). This value was subtracted from other rates to give the ATPase activity of reverse gyrase of 20 ± 3 s^{-1} with bubbled DNA ($n = 3$), 4.8 s^{-1} with ssDNA ($n = 1$), and 0.0 ± 0.3 s^{-1} without DNA ($n = 2$).

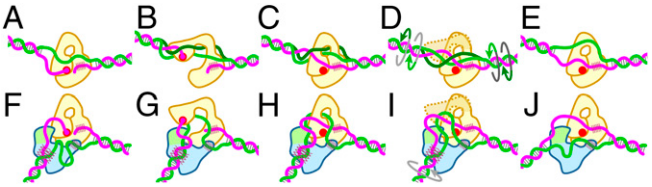

Fig. 7. Chiral operation by reverse gyrase. (*A*–*E*) Presumed mechanism of passive strand passage in topo IA. The magenta strand is held (hatched) in a groove. (*A*) Catalytic tyrosine (red circle) cuts the strand and binds one end. (*B*) Thermal opening of the gate to the central cavity allows thermal strand passage in either direction (light or dark green). (*C*) When the gate closes and the cut strand happens to be religated, the Lk has changed by one (ΔLk = ±1). (*D*) Reopening of the gate without strand scission allows the green strand to exit from the cavity. The ΔLk localized in the ss region is spread (diluted) into the entire DNA through rotation of the ss/ds junction. (*E*) Enzyme is then ready for another passage. All events are stochastic and reversible. (*F*–*J*) In reverse gyrase, gate opening is likely controlled by ATP hydrolysis in the helicase domain (light blue) through the latch domain (light green). Biased strand passage may occur as follows. The ds/ss junction on the scissile side (*F*, *Left*) and a distant part of the green strand (*F*, *Right*) are both bound to the enzyme. (*G*) Coupled to unlocking of gate motion, the ds region elongates by base pairing, rotating the two ss ends to bias the passage correctly. Religation occurs while the bias is effective (*H*), and the green strand exits with ΔLk = +1 (*I*). The gate is locked, and DNA is allowed to rotate to export the ΔLk (*I*→*J*). The export would fail if the DNA were already highly overwound. Many variations of this scheme are possible.

Reverse gyrase sharply slows down as Γ approaches Γ_c (Fig. 5*B*). In bulk assays with circular DNA, Γ increases as more supercoils are introduced. The bulk result above of ΔLk = 10 implies an Lk density σ of ~0.03. For this σ, theory (30) predicts a torsional stress of ~5 pN·nm at no tension (plasmids do not bear tension). This value agrees with our experimental Γ_c, explaining why the bulk activity near the end point was so low. There was a sign of a faster phase, but quantification is difficult in gel analyses. In any event, the kinetic features revealed here, quick overwinding at low torsional stress and sharp cessation at a moderate stress, aptly suit the physiological role of reverse gyrase if the demand is to keep DNA slightly overwound to protect, but not overprotect, the genome of hyperthermophiles against thermal denaturation and to restore the protected state quickly after thermal or replication/transcription-related perturbations.

The rather small Γ_c that limits the reverse gyrase activity is as expected if the strand passage mechanism in reverse gyrase is basically the same as the strand passage mechanism in genuine topo IA (5) (Fig. 7 *A*–*E*). In topo IA, strand passage is a passive process relying on thermal fluctuations of the strand and the enzyme. The preference between the two modes of passage (light or dark green in Fig. 7*C*) is determined by the overall torsional stress in the DNA; thus, on average, the reaction tends to relax the DNA (Lk approaches Lk_0). Reverse gyrase, in contrast, must increase Lk beyond Lk_0 by actively biasing the direction of strand passage. In one proposal (5) for circular DNA, binding of reverse gyrase to DNA induces local DNA unwinding, whereas the rest of DNA is overwound. ATP then allows topoisomerase action on the unwound region to increase the Lk by 1. In this model, correct bias comes from the initial unwinding and the restoring pressure from the overwound region. In our bubbled linear DNA, however, the substrate site is unwound from the beginning and bead rotation cancels overwinding. Wrapping of DNA around reverse gyrase could also provide a bias (12), but whether it works with a bubble is not clear. Models starting with thermally melted DNA (7, 31) are readily compatible with our bubble results. Bias may originate from binding of the double-stranded (ds) or ss region in a specific manner (7) or by alternation of ss and ds bindings (31).

Here, we show a variant of the latter in Fig. 7 *F–J*, without compelling evidence. The bias comes from base pairing at the ds/ss junction, as would happen as a reversal of the duplex unwinding shown for the helicase domain (32). The pairing rotates the ends of the two single strands to bias strand passage correctly. During passage, all four ends of the two single strands are bound to the enzyme to isolate the ss region from the stress in the rest of DNA. After passage, however, the positive twist in the ss region must be exported to the entire DNA. This process is sensitive to the torsional stress in the entire DNA, and it fails when the opposing stress is too high. If the opposing stress exceeds Γ_c, the model predicts underwinding, which we indeed observed (Fig. S5). A priori, the enzyme could work against a high stress if the active bias might somehow accumulate over successive cycles. For the accumulation, all four ends must always be under control and continuously twisted as in a hand-over-hand fashion, a mechanism not readily conceivable in the known structures of reverse gyrase. Perhaps there is no physiological need for excessive overwinding, which would actually be harmful.

The mechanism above relying on stochastic thermal motions implies loose coupling with ATP hydrolysis, which we indeed observed. Unlocking of the gate by ATP hydrolysis does not necessarily accompany strand passage, and the passage may occasionally occur in the wrong direction. The wrong bias is the norm when exposed to torsional stress exceeding Γ_c (Fig. S5), implying that after reaching Γ_c, reverse gyrase would continue vain cycles either forward or backward with equal probability, consuming ATP.

The high tension dependence with the unusually large interaction length δ of ~32 nm, far exceeding the dimension of reverse gyrase of ~13 nm (12), is also consistent with the above mechanism. A large value of ~10 nm has also been reported for topo IA working on a bubbled DNA (20). Threading the green strand through the cavity (Fig. 7) would require an extra length compared with the magenta strand. Indeed, topo IA working on a bulged substrate, where one ss arm was much longer than the other, was insensitive to tension (20). In reverse gyrase, in addition, all four ends of the two strands must be bound for biased passage while the two ss portions are sufficiently slack. Holding four ends likely requires overall bending of the DNA, as in Fig. 7. Tension thus impedes the operation of reverse gyrase.

Methods

Reverse gyrase was purified from *S. tokodaii* as described (4). The bubbled DNA substrates shown in Fig. 1*A* were prepared as in Fig. S1, appending multiply biotinylated and digoxigenin-labeled ends. The biotinylated ends were attached to a coverslip modified with biotinylated polyethylene glycol. We attached to the other ends carboxylated superparamagnetic beads (1-μm diameter) coated with antidigoxigenin antibody. For the rotation experiments in Figs. 2 and 3, we added fluorescent daughter beads (0.2-μm diameter), which we found to bind to the magnetic beads. Assays were made in 50 mM Tris·HCl (pH 7.9 at 23 °C) containing 0.1 mM EDTA, 50 mM NaCl, 10 mM $MgCl_2$, 5 mM DTT, 5 mM ATP, and 0.001–10 nM reverse gyrase. The beads were observed on an inverted microscope, and images were recorded at 30 Hz. For rapid temperature control, two circulating water baths set at desired temperatures were connected alternately to water channels inside the copper sample holder and copper objective jacket (Fig. 1*B*). The magnetic beads were pulled upward with a single neodymium magnet (Fig. 1*D*) or a pair of neodymium magnets (Figs. 1*C* and 4*A*). The vertical pulling force F was calibrated by tethering the magnetic bead with 16.5-μm-long λ-phage DNA and measuring at 23 °C the amplitude of the Brownian fluctuations of the bead. Bead-sinking assays in Fig. 4 were basically as described by Strick et al. (19). We estimated the bead height z from the diffraction pattern in the defocused bead image (Fig. S3). ATP hydrolysis was assayed in the same solution as above by monitoring ADP production with reverse phase chromatography. Detailed materials and methods are presented in *SI Methods*.

ACKNOWLEDGMENTS. We thank M. Shio and K. Fujino for the stable microscope stage; Ke. Adachi for image analysis programs; members of the K.K. laboratory for technical advice and discussion; and Ku. Adachi, S. Takahashi, K. Sakamaki, and M. Fukatsu for encouragement and laboratory management. This work was supported by Monbukagakusho/Japan Society for the Promotion of Science Kakenhi Grants 16002013, 21000011, and 26221102.

1. Kikuchi A, Asai K (1984) Reverse gyrase—A topoisomerase which introduces positive superhelical turns into DNA. *Nature* 309(5970):677–681.
2. Suzuki T, et al. (2002) *Sulfolobus tokodaii* sp. nov. (f. *Sulfolobus* sp. strain 7), a new member of the genus *Sulfolobus* isolated from Beppu Hot Springs, Japan. *Extremophiles* 6(1):39–44.
3. Forterre P, Mirambeau G, Jaxel C, Nadal M, Duguet M (1985) High positive supercoiling *in vitro* catalyzed by an ATP and polyethylene glycol-stimulated topoisomerase from *Sulfolobus acidocaldarius*. *EMBO J* 4(8):2123–2128.
4. Nakasu S, Kikuchi A (1985) Reverse gyrase; ATP-dependent type I topoisomerase from *Sulfolobus*. *EMBO J* 4(10):2705–2710.
5. Serre MC, Duguet M (2003) Enzymes that cleave and religate DNA at high temperature: The same story with different actors. *Prog Nucleic Acid Res Mol Biol* 74:37–81.
6. Nadal M (2007) Reverse gyrase: An insight into the role of DNA-topoisomerases. *Biochimie* 89(4):447–455.
7. Lulchev P, Klostermeier D (2014) Reverse gyrase—Recent advances and current mechanistic understanding of positive DNA supercoiling. *Nucleic Acids Res* 42(13):8200–8213.
8. Mirambeau G, Duguet M, Forterre P (1984) ATP-dependent DNA topoisomerase from the archaebacterium *Sulfolobus acidocaldarius*. Relaxation of supercoiled DNA at high temperature. *J Mol Biol* 179(3):559–563.
9. López-García P, Forterre P (1999) Control of DNA topology during thermal stress in hyperthermophilic archaea: DNA topoisomerase levels, activities and induced thermotolerance during heat and cold shock in *Sulfolobus*. *Mol Microbiol* 33(4):766–777.
10. Confalonieri F, et al. (1993) Reverse gyrase: A helicase-like domain and a type I topoisomerase in the same polypeptide. *Proc Natl Acad Sci USA* 90(10):4753–4757.
11. Déclais AC, Marsault J, Confalonieri F, de La Tour CB, Duguet M (2000) Reverse gyrase, the two domains intimately cooperate to promote positive supercoiling. *J Biol Chem* 275(26):19498–19504.
12. Rodríguez AC, Stock D (2002) Crystal structure of reverse gyrase: Insights into the positive supercoiling of DNA. *EMBO J* 21(3):418–426.
13. Rudolph MG, del Toro Duany Y, Jungblut SP, Ganguly A, Klostermeier D (2013) Crystal structures of *Thermotoga maritima* reverse gyrase: Inferences for the mechanism of positive DNA supercoiling. *Nucleic Acids Res* 41(2):1058–1070.
14. Shibata T, Nakasu S, Yasui K, Kikuchi A (1987) Intrinsic DNA-dependent ATPase activity of reverse gyrase. *J Biol Chem* 262(22):10419–10421.
15. Hsieh TS, Capp C (2005) Nucleotide- and stoichiometry-dependent DNA supercoiling by reverse gyrase. *J Biol Chem* 280(21):20467–20475.
16. Slesarev AI, Kozyavkin SA (1990) DNA substrate specificity of reverse gyrase from extremely thermophilic archaebacteria. *J Biomol Struct Dyn* 7(4):935–942.
17. Hsieh TS, Plank JL (2006) Reverse gyrase functions as a DNA renaturase: Annealing of complementary single-stranded circles and positive supercoiling of a bubble substrate. *J Biol Chem* 281(9):5640–5647.
18. Rodríguez AC (2003) Investigating the role of the latch in the positive supercoiling mechanism of reverse gyrase. *Biochemistry* 42(20):5993–6004.
19. Strick TR, Croquette V, Bensimon D (2000) Single-molecule analysis of DNA uncoiling by a type II topoisomerase. *Nature* 404(6780):901–904.
20. Dekker NH, et al. (2002) The mechanism of type IA topoisomerases. *Proc Natl Acad Sci USA* 99(19):12126–12131.
21. Gore J, et al. (2006) Mechanochemical analysis of DNA gyrase using rotor bead tracking. *Nature* 439(7072):100–104.
22. Terekhova K, Gunn KH, Marko JF, Mondragón A (2012) Bacterial topoisomerase I and topoisomerase III relax supercoiled DNA via distinct pathways. *Nucleic Acids Res* 40(20):10432–10440.
23. Yogo K, et al. (2012) Direct observation of strand passage by DNA-topoisomerase and its limited processivity. *PLoS ONE* 7(4):e34920.
24. Revyakin A, Ebright RH, Strick TR (2005) Single-molecule DNA nanomanipulation: Improved resolution through use of shorter DNA fragments. *Nat Methods* 2(2):127–138.
25. Lipfert J, Wiggin M, Kerssemakers JW, Pedaci F, Dekker NH (2011) Freely orbiting magnetic tweezers to directly monitor changes in the twist of nucleic acids. *Nat Commun* 2:439.
26. Duguet M (1993) The helical repeat of DNA at high temperature. *Nucleic Acids Res* 21(3):463–468.
27. Jaxel C, et al. (1989) Reverse gyrase binding to DNA alters the double helix structure and produces single-strand cleavage in the absence of ATP. *EMBO J* 8(10):3135–3139.
28. Mosconi F, Allemand JF, Bensimon D, Croquette V (2009) Measurement of the torque on a single stretched and twisted DNA using magnetic tweezers. *Phys Rev Lett* 102(7):078301.
29. Clauvelin N, Audoly B, Neukirch S (2008) Mechanical response of plectonemic DNA: An analytical solution. *Macromolecules* 41(12):4479–4483.
30. Marko JF (2007) Torque and dynamics of linking number relaxation in stretched supercoiled DNA. *Phys Rev E Stat Nonlin Soft Matter Phys* 76(2 Pt 1):021926.
31. Plank J, Hsieh TS (2009) Helicase-appended topoisomerases: New insight into the mechanism of directional strand transfer. *J Biol Chem* 284(45):30737–30741.
32. Ganguly A, del Toro Duany Y, Klostermeier D (2013) Reverse gyrase transiently unwinds double-stranded DNA in an ATP-dependent reaction. *J Mol Biol* 425(1):32–40.

Supporting Information

Ogawa et al. 10.1073/pnas.1422203112

SI Methods

Enzyme. Reverse gyrase was purified from *S. tokodaii* as described (1).

DNA Constructs. The bubbled DNA substrates shown in Fig. 1*A* were prepared by annealing a complementary ssDNA pair containing a 30-nt mismatch essentially as described by Hsieh and Plank (2) and appending a biotinylated fragment and a digoxigenin-labeled fragment at each end following the method of Revyakin et al. (3). Details are provided in the legend for Fig. S1.

Observation Chamber. Coverslips were modified with biotinylated PEG for DNA attachment and surface blocking. First, we coated $18 \times 18\text{-mm}^2$ (for chamber top) and $24 \times 32\text{-mm}^2$ (for chamber bottom) coverslips (Matsunami Glass) with (3-mercaptopropyl) trimethoxysilane (Momentive Performance Materials) and reduced the SH groups with DTT basically as described (4). We then sandwiched between pairs of top coverslips 10 mM methyl-PEG-maleimide [molecular weight (MW) of 700; Thermo Scientific] in 50 mM 3-(*N*-morpholino)propanesulfonic acid-NaOH (pH 7.0) and incubated the coverslips overnight at room temperature. The reagent for the chamber bottom contained in addition 0.1 mM biotin-PEG-maleimide (MW of 600; Quanta Bio Design). Finally, we washed the coverslips with water and stored them in water at 4 °C until use.

A flow chamber with a side chamber for a thermocouple (Fig. 1*B*) was made of the modified coverslips separated by three strips of double-sided tape of 80-μm thickness (300A80B; Kyodo Giken Kagaku). We infused one chamber volume (~10 μL) of 1 mg/mL streptavidin (Pierce) in buffer A [10 mM Tris·HCl (pH 7.9), 1 mM EDTA, 50 mM NaCl] into the main chamber, waited for 10 min, and washed out unbound streptavidin with 10 vol of buffer A. Further infusion and incubation were as follows: two chamber volumes of a DNA substrate at ~20 pM in buffer A (5 min); 2 vol of 10 mg/mL biotin-PEG (MW of 5,000; Laysan Bio) in buffer A for blocking unreacted streptavidin on the surface (5 min); 1 vol of carboxylated superparamagnetic beads (1-μm diameter; Dynal) that had been coated with antidigoxigenin antibody (polyclonal; Acris Antibodies) and methyl-PEG-amine (MW of 1,100; Quanta BioDesign) by cross-linking with EDC and sulfo-NHS (Pierce) as described (5) and suspended at $\sim 5 \times 10^8$ particles per milliliter in buffer A (10 min); 5 vol of fluorescent daughter beads (0.2-μm diameter, Red; Molecular Probes), which were found to bind to the magnetic beads, at $\sim 2 \times 10^9$ particles per milliliter in buffer A (5 min); 5 vol of buffer B [50 mM Tris·HCl (pH 7.9 at 23 °C), 0.1 mM EDTA, 50 mM NaCl, 10 mM $MgCl_2$, 5 mM DTT, 5 mM ATP]; and 5 vol of 0.001–10 nM reverse gyrase in buffer B. Finally, we sealed the main chamber with quick dry epoxy (Debcon) and the side chamber with silicone grease. During the infusions (at room temperature), the chamber was placed under a 5-G magnetic field to help align the magnetic beads vertically. This magnet and fluorescent beads were omitted in the plectoneme assays shown in Fig. 4. For dilution of the enzyme stock, we used nonadsorbing tips and tubes.

Microscopy. Samples were observed on an inverted microscope (IX71 or IX73; Olympus) with a 100× oil-immersion objective (UPALSAPO100X; Olympus). Fluorescent daughter beads were observed with standard epifluorescence optics consisting of a mercury lamp and a mirror unit (U-MWIG3; Olympus), and magnetic beads were illuminated with ring-type light-emitting diodes (Moritex). Images were captured with an EM-CCD camera (ADT-33B; Flovel) at 30 Hz and recorded on a hard disk with VideoSavant 4.0 software (IO Industries). Bead rotation was analyzed by tracing the centroid of a fluorescent daughter bead (6).

To control the sample temperature, we placed a copper-made custom holder (Fig. 1*B*) on a stable microscope stage (KS-O; ChuukoushaSeisakujo) and attached a tightly fitted copper jacket on the objective. For rapid temperature control, two circulating water baths set at desired temperatures were connected alternately to the water channels inside the holder and jacket. The sample temperature was monitored with a thermocouple (K type, 50-μm diameter; Ishikawa Sangyo) in the side chamber at a distance of ~5 mm from the observed area and recorded on a data logger (TC-08; Pico Technology) synchronously with the video images. When we placed another thermocouple in the main chamber, the two agreed within ±1 °C.

A neodymium cylinder magnet, with a diameter of 10 mm and height of 10 mm with a conical iron headpiece 3 mm high (Fig. 1*D*), was placed above the sample to pull the bead (7). The vertical pulling force F was calibrated by tethering the magnetic bead with 16.5-μm-long λ-phage DNA and measuring at 23 °C the amplitude of the Brownian fluctuations of the bead (8). We used a water immersion lens to estimate the bead height z from the movement of the objective needed for focusing and recorded the bead position (x, y) for 5 min at 60 frames per second at 23 °C. We estimated the tension as $F = 2k_BTz/(\delta x^2 + \delta y^2)$, where the thermal energy k_BT was taken as 4.1 pN·nm and δx^2 and δy^2 are variances of the bead position.

To control the bead orientation (Fig. 4), we used a pair of neodymium square magnets ($8 \times 8 \times 6\ \text{mm}^3$) separated by a 1-mm gap and mounted on a motor-controlled holder. Because the focus drift was appreciable at 71 °C, we included in the sample biotinylated 2-μm beads, which were tightly bound to the streptavidin-coated surface and served as a height reference. We illuminated both the magnetic and reference beads through the narrow gap between the magnets and deliberately defocused the bead image to estimate the bead height z from the diffraction pattern (9) (Fig. S3*A*). We estimated the size of the first diffraction ring by fitting its intensity distribution with a circle with a Gaussian radial profile. To convert the ring size to z, we imaged surface-stuck magnetic beads and reference beads at various focal positions. This calibration was made with the water and oil immersion objectives; for the latter, we corrected the apparent height (distance moved by the objective) for the refraction at the water/glass interface by multiplication by 1.15 = 1.52/1.33, the ratio of refractive indices of glass and water. The narrow illumination would ensure this simple correction. We measured the vertical pulling force F of the magnet pair with the λ-DNA as above and fitted the force (F) − extension (z) data with the worm-like chain model (10). The estimated persistence length and contour length at 23 °C in buffer A containing 5 mM DTT were 56.6 nm and 16.4 μm with water immersion and 56.3 nm and 16.3 μm with oil, which are in reasonable agreement. We applied the same height correction in the reverse gyrase assays using the oil-immersion objective (Fig. 4), ignoring the temperature dependence of the refractive indices. The origin of z ($z = 0$ when the bead sits on the surface) was taken close to the lowest points in the unfiltered time course for each measurement. In rare instances, a bead attached to the surface and ceased fluctuation. From these events, we estimate the precision in the z origin to be ±0.05 μm.

ATPase Activity. ATP hydrolysis by reverse gyrase was assayed as described (11). For this experiment, we prepared two essentially

complementary 147-mer oligonucleotides copied from the mid-bubble DNA except for the bubble portion. One was used as ssDNA. Annealing of the two produced 143-mer dsDNA with a 30-nt central bubble and 4-nt ss tails (Fig. S4*E*). We started an assay by incubating 10 nM reverse gyrase at 71 °C in buffer B (−ATP) without or with 100 nM DNA. The solution was capped with mineral oil to avoid evaporation. After 5 min, we started the reaction by adding ATP to the final concentration of 5 mM. At intervals (0, 5, 10, 30, 60, and 120 min), a 20-μL aliquot was drawn and quenched by ice-cold perchloric acid (final = 0.1 M). After centrifugation, the mixture was neutralized with cold NaOH and analyzed by reverse phase chromatography (ODS-100V; Tosoh) as detailed in the legend for Fig. S4.

1. Nakasu S, Kikuchi A (1985) Reverse gyrase; ATP-dependent type I topoisomerase from *Sulfolobus*. *EMBO J* 4(10):2705–2710.
2. Hsieh TS, Plank JL (2006) Reverse gyrase functions as a DNA renaturase: Annealing of complementary single-stranded circles and positive supercoiling of a bubble substrate. *J Biol Chem* 281(9):5640–5647.
3. Revyakin A, Ebright RH, Strick TR (2005) Single-molecule DNA nanomanipulation: Improved resolution through use of shorter DNA fragments. *Nat Methods* 2(2):127–138.
4. Itoh H, et al. (2004) Mechanically driven ATP synthesis by F_1-ATPase. *Nature* 427(6973):465–468.
5. Kim S, Blainey PC, Schroeder CM, Xie XS (2007) Multiplexed single-molecule assay for enzymatic activity on flow-stretched DNA. *Nat Methods* 4(5):397–399.
6. Yasuda R, Noji H, Yoshida M, Kinosita K, Jr, Itoh H (2001) Resolution of distinct rotational substeps by submillisecond kinetic analysis of F_1-ATPase. *Nature* 410(6831):898–904.
7. Harada Y, et al. (2001) Direct observation of DNA rotation during transcription by *Escherichia coli* RNA polymerase. *Nature* 409(6816):113–115.
8. Strick TR, Allemand JF, Bensimon D, Bensimon A, Croquette V (1996) The elasticity of a single supercoiled DNA molecule. *Science* 271(5257):1835–1837.
9. Gosse C, Croquette V (2002) Magnetic tweezers: Micromanipulation and force measurement at the molecular level. *Biophys J* 82(6):3314–3329.
10. Bustamante C, Marko JF, Siggia ED, Smith S (1994) Entropic elasticity of λ-phage DNA. *Science* 265(5178):1599–1600.
11. Jungblut SP, Klostermeier D (2007) Adenosine 5′-O-(3-thio)triphosphate (ATPgammaS) promotes positive supercoiling of DNA by T. maritima reverse gyrase. *J Mol Biol* 371(1):197–209.

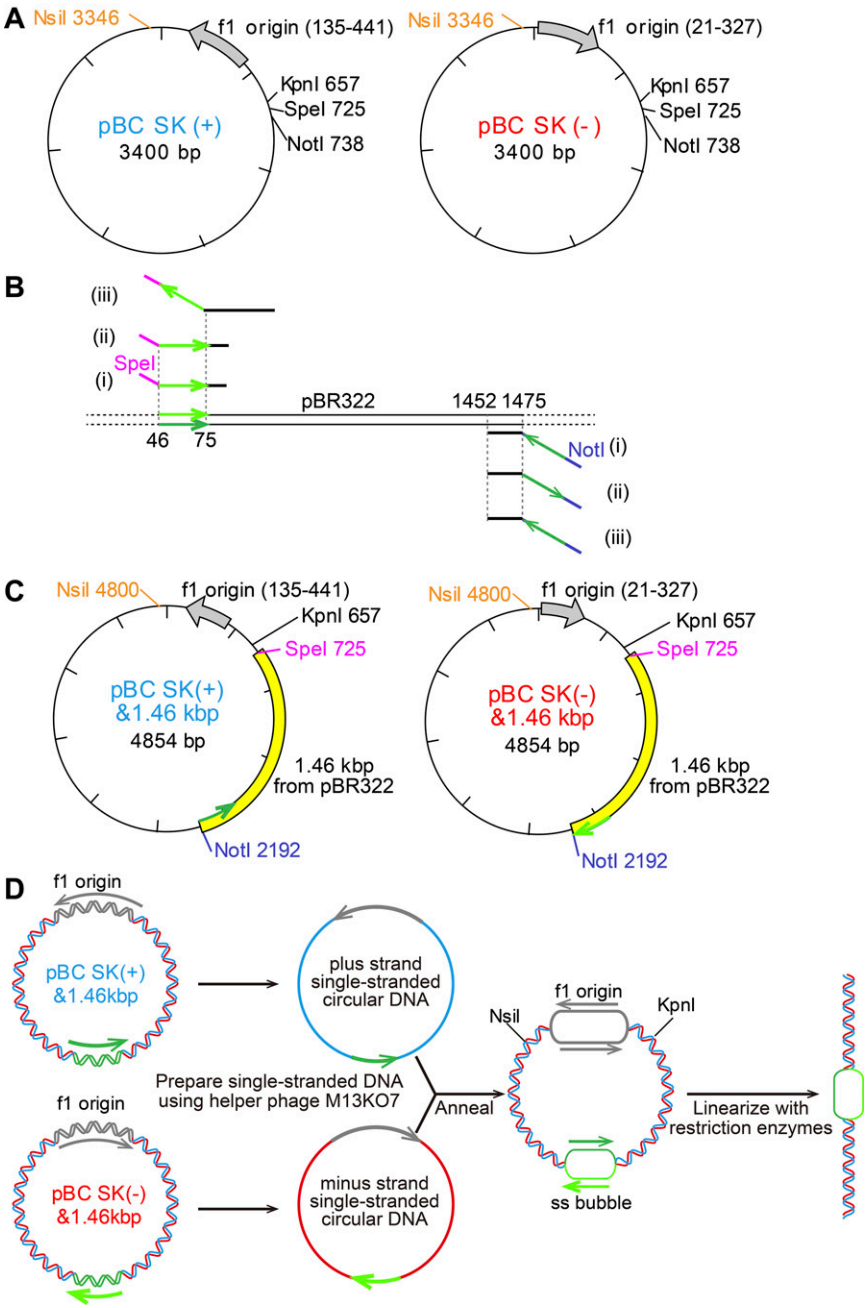

Fig. S1. Preparation of DNA substrates. The bubbled DNA substrates shown in Fig. 1*A* were prepared by annealing a complementary ssDNA pair containing a 30-nt mismatch essentially as described (1) and appending a biotinylated fragment and a digoxigenin (DIG)-labeled fragment at each end (2). (*A*) To prepare the ssDNA pair, we first introduced an NsiI site at 3,346 in pBC SK(+) and pBC SK(–) phagemid vectors (Stratagene), which contain an ssDNA replication origin (f1) in the (+) or (–) orientation. (*B*) To construct the 30-nt bubble shown in Fig. 1*A*, we prepared from pBR322 three kinds of 1.46-kbp fragments flanked by SpeI and NotI sites, using the primer pairs i–iii. The green arrows show the pBR322 sequence from 46 to 75 in this direction, with light and dark colors distinguishing the two complementary strands. (*C*) For the mid-bubble substrate, the 1.46-kbp fragments prepared by primer pairs i and ii were each introduced into pBC SK(+) and pBC SK(–), respectively, between the SpeI and NotI sites. The NotI ends of the two constructs differed in polarity (green arrows are shown for the strand that will be copied by helper phase in *D*). For the end bubble, we used primer pairs i and iii, resulting in opposite polarities on the SpeI ends. (*D*) We added helper phage M13KO7 (New England Biolabs), which is a derivative of M13 bacteriophage, to each construct to obtain ssDNA dictated by the f1 origin. The ssDNA pair (cyan and red) was annealed and linked by reverse gyrase in the presence of ADP. Finally, we digested the circular dsDNA with NsiI and KpnI to obtain a linear duplex with a bubble. For the control DNA without a bubble, we simply digested the left construct in *C*. To add a biotinylated end to the obtained linear DNA duplexes, we prepared a 1-kbp fragment with PCR using pBC SK(+) as a template (upstream from NsiI) and an equimolar mixture of biotin-labeled dUTP and nonlabeled dNTP. A 1-kb DIG-labeled end was prepared similarly from the downstream sequence from KpnI. The biotin- and DIG-labeled 1-kb ends were then ligated to the NsiI-KpnI fragment as described by Revyakin et al. (2).

1. Hsieh TS, Plank JL (2006) Reverse gyrase functions as a DNA renaturase: Annealing of complementary single-stranded circles and positive supercoiling of a bubble substrate. *J Biol Chem* 281(9):5640–5647.
2. Revyakin A, Ebright RH, Strick TR (2005) Single-molecule DNA nanomanipulation: Improved resolution through use of shorter DNA fragments. *Nat Methods* 2(2):127–138.

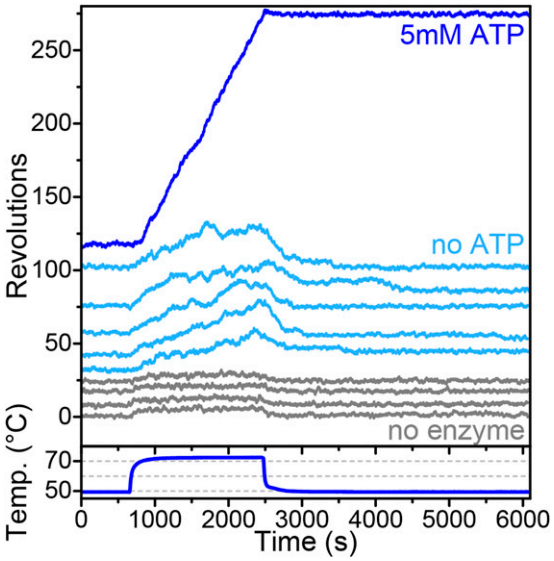

Fig. S2. DNA unwinding by binding of reverse gyrase in the absence of ATP. A long-time version of the experiments in Fig. 2*B* (*Left*) is shown. A bead tethered by the nonbubble DNA was observed under 0.5 pN of tension in the presence of 10 nM reverse gyrase. The slow rotation at 71–72 °C in the absence of ATP is reversed upon cooling to 50 °C. The interpretation is that thermal unwinding of DNA is progressively stabilized by successive binding of reverse gyrase and, upon cooling, renaturation proceeds following stochastic unbinding of reverse gyrase. At 71–72 °C, unwinding continues because already melted regions are stabilized by reverse gyrase, whereas the rest of DNA is kept relaxed by bead rotation, allowing further melting. Such unwinding cannot take place in a circular plasmid, but if the DNA is nicked, reverse gyrase can unwind the plasmid DNA in the absence of ATP (1). (*Top*) In our bead rotation assay in the presence of ATP, the bead rotated faster, as shown in this trace. This rotation must be caused by genuine overwinding activity of reverse gyrase, because the introduced turns remained after cooling.

1. Jaxel C, et al. (1989) Reverse gyrase binding to DNA alters the double helix structure and produces single-strand cleavage in the absence of ATP. *EMBO J* 8(10):3135–3139.

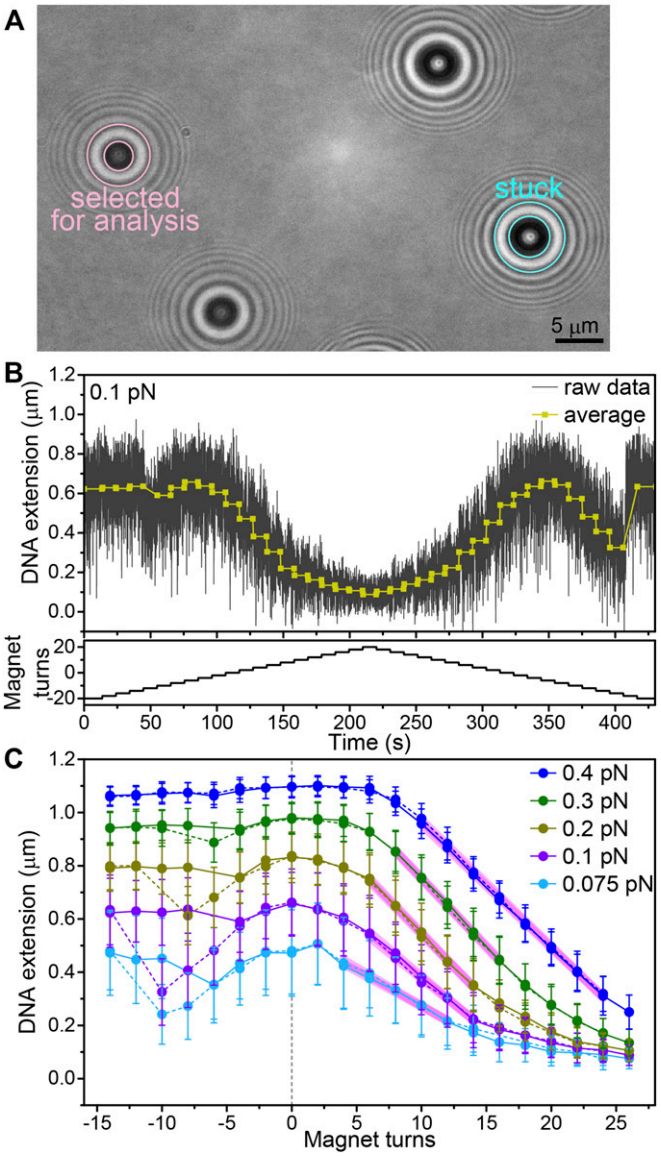

Fig. S3. Dependence of DNA extension on twist turns. (*A*) Snapshot of tethered 1-μm beads and a surface-stuck 2-μm bead. We slightly defocus the image such that diffraction rings show up. The first ring between two concentric circles is fitted with a circle with a Gaussian radial profile. The ring diameter thus estimated is converted to the bead height on the basis of separate calibration. (*B*) Partial time course of extension-rotation measurement. At each tension, we rotate a bead from −20 turns to +20 turns and back to −20 turns in steps of two turns with 10-s pause in between. The return cycle is then repeated at a different tension. The average bead height and the fluctuation amplitude (SD) during each 10-s pause are recorded. The erratic behaviors at the beginning and end of this time course are due to thermal melting and renaturation of the DNA, as explained in *C*. (*C*) DNA extension (bead height) against twist turns (*m*). Solid lines represent measurements from negative to positive turns, and dashed lines represent measurements back to negative. Error bars show SD for thermal fluctuations over 10 s. In Fig. 4*B* (*Right*), we only show the results of positive-to-negative excursions. The mid-bubble DNA at 71 °C in the absence of reverse gyrase is shown. The highest extensions are assigned to $m = 0$ (fully relaxed state). On the negative (unwinding) side, the extension tends to remain high particularly at higher tensions. This tendency is due to partial melting of underwound DNA, which requires >0.5 pN of tension at room temperature (1). At 71 °C here, DNA melts more readily and renaturation also takes place at low tensions, leading to the instability seen in *B*. Measurements interrupted by these instabilities (and by rare attachment of the bead to the glass surface) are omitted from this graph. On the positive (overwinding) side, which is related to the reverse gyrase activity, we estimate the slope of the linear portion by fitting a straight line (magenta) to the segment starting at 90% of the highest extension and ending at 30% or 0.2 μm, whichever is higher. Seven beads (8–12 slopes because not all measurements were successful) gave consistent results: 31 ± 5 nm per turn at 0.075 pN, 41 ± 3 nm per turn at 0.1 pN, 47 ± 5 nm per turn at 0.2 pN, 49 ± 3 nm per turn at 0.3 pN, and 46 ± 1 nm per turn at 0.4 pN. These average values are used for the estimations of reaction rates and required torque.

1. Strick T, Allemand JF, Bensimon D, Lavery R, Croquette V (1999) Phase coexistence in a single DNA molecule. *Physica A* 263(1-4):392–404.

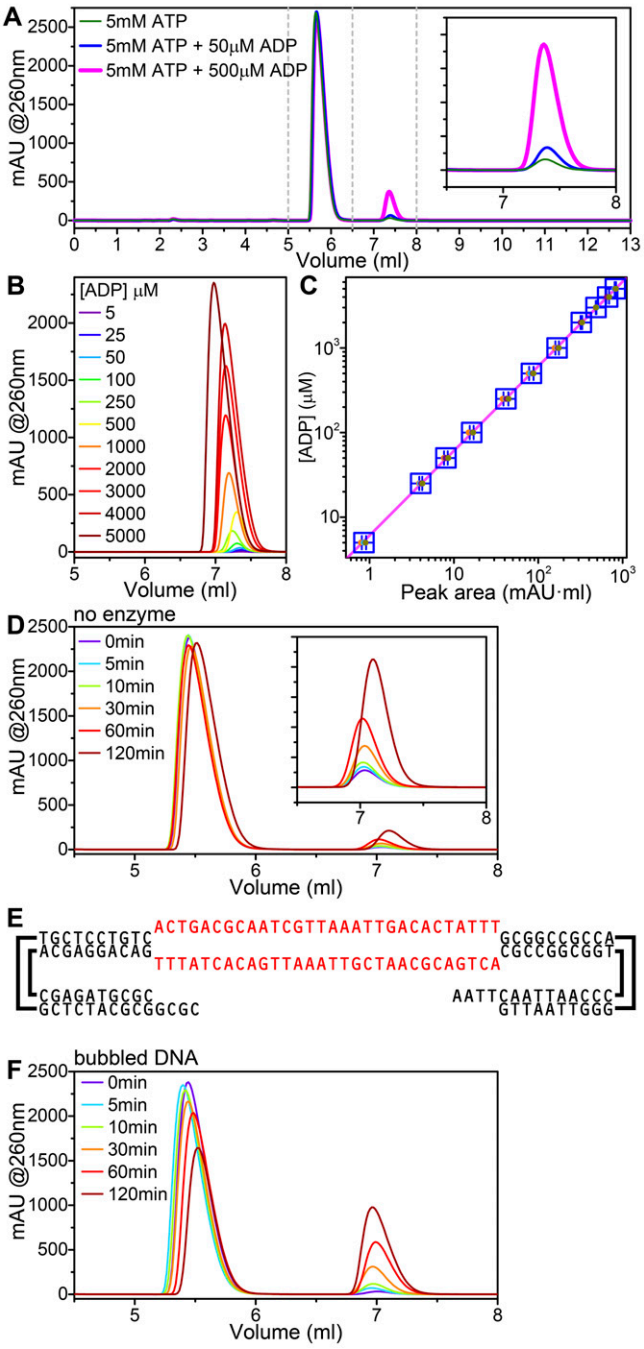

Fig. S4. ATP hydrolysis assay. (*A*) Separation of ATP and ADP by reverse phase chromatography. The ATP peak appears between 5 and 6.5 mL, and the ADP peak appears between 6.5 and 8 mL, which is magnified (*Inset*). The ATP we used contained ~1% ADP, which was corrected for in the hydrolysis assays below. mAU, milli absorbance unit. (*B* and *C*) Calibration with known concentrations of ADP. The ADP had been purified with a MonoQ 5/50 GL column (GE Healthcare), showing no trace of ATP. The peak area between 6.5 and 8 mL was used to quantify ADP. (*D*) Hydrolysis of 5 mM ATP at 71 °C in the absence of reverse gyrase. The assay was performed as described in *SI Methods*, omitting reverse gyrase. The hydrolysis rate estimated in three samples (Fig. 6) averaged 2.3 ± 0.1 μM ATP per minute per 5 mM ATP = $(4.6 \pm 0.2) \times 10^{-4}$ min^{-1} in buffer B at 71 °C, close to the literature value at 70 °C and pH 7.6 in the presence of Mg^{2+} of 3.82×10^{-4} min^{-1} (1). We did not detect an ADP increase over 1 h of incubation at room temperature. (*E*) Bubbled DNA used in the ATPase assay. The bubble here is a combination of one bubble strand in Fig. 1*A* and its reversed sequence. (*F*) Hydrolysis of 5 mM ATP by 10 nM reverse gyrase in the presence of 100 nM bubbled DNA. The assay at 71 °C was performed as in *SI Methods*. Three samples gave an average hydrolysis rate of 14.3 ± 1.6 μM·min^{-1}, from which the rate in the absence of the enzyme in *D* was subtracted to give the ATPase activity as 20 ± 3 s^{-1} (Fig. 6).

1. Ramirez F, Marecek JF, Szamosi J (1980) Magnesium and calcium ion effects on hydrolysis rates of adenosine 5′-triphosphate. *J Org Chem* 45(23):4748–4752.

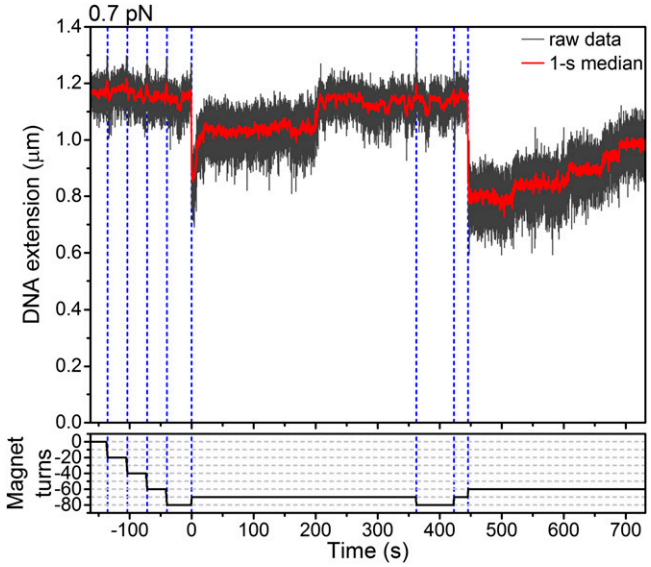

Fig. S5. Relaxation of positive supercoils at high tension. With the experimental setup in Fig. 4, we applied 0.7 pN of tension to the DNA in the presence of 1 nM reverse gyrase. Under this high tension, unwinding maneuvers by 20 turns with magnets did not change the bead height (before 0 s). Presumably, reverse gyrase relaxed the introduced negative torsions and, by time 0, wound the DNA to a slightly overwound state. Thus, only 10 positive turns with magnets at 0 s brought down the bead appreciably. The downward movement must be due to the introduction by magnets of plectonemes (positive supercoils), which required ~8 pN·nm of torque under 0.7 pN of tension. This high torsional stress exceeding Γ_c of ~5 pN·nm let reverse gyrase work in reverse: The bead rose to the original height in two steps, showing relaxation of positive supercoils by reverse gyrase. From ~360 s, we repeated similar maneuvers. In this trial, the first positive 10 turns at ~420 s failed to sink the bead, indicating that reverse gyrase had not yet overwound the DNA sufficiently, but the second 10 turns at ~445 s brought the bead down. Thereafter the bead again rose toward the original height, indicating relaxation of positive supercoils. We could repeat such maneuvers several times on the same bead, showing that the rise of the bead was not due to DNA nicking. The relaxation kinetics varied from trial to trial and from bead to bead.

Movie S1. Rotation of a fluorescent daughter bead in response to DNA overwinding by reverse gyrase. The portion between 1,722 and 1,823 s of the red curve in Fig. 2*B* is shown. The experiment was with 10 nM reverse gyrase and mid-bubble DNA at 71 °C. The image size is 3.6 × 3.6 μm^2.

Movie S1